TRACOR Document No.
T72-AU-9597-U

MOST Project -1

IR & D REPORT

EXTENSION OF THE TARGET STRENGTH STUDIES

by

B. M. Brown and Geoffrey Maltin

20 October 1972

TRACOR

6500 Tracor Lane, Austin, Texas 78721, AC 512/926-2800

TRACOR 6500 TRACOR LANE, AUSTIN, TEXAS 78721

ROUGH DRAFT

TRACOR-Document No.
T72-AU-9597-U

IR & D REPORT,

EXTENSION OF THE TARGET STRENGTH STUDIES,

by

B. M. Brown and Geoffrey Maltin

20 October 1972

33 p.

Approved:

W. C. Moyer
W. C. Moyer
Assistant Vice President

352 100

TABLE OF CONTENTS

LIST OF ILLUSTRATIONS

LIST OF TABLES

I. INTRODUCTION

A method to predict accurately the sonar target strength and signature of a submarine would be a valuable tool to a designer. It could substitute for many costly experiments, guide the designer toward a proper design, and give reasonable assurance that the submarine, when built, would have a desirably small sonar cross section. To attain such a method, TRACOR, in 1964, began an investigation of this problem. A theory was developed and implemented through a computer program. The results can be found in Ref. 1.

In the model created to simulate this problem the hull structure was approximated by an ellipse of revolution. To this was added a rectangular box with half cylinders on the fore and aft ends to represent the sail. This constituted the geometrical representation of the submarine. The reflections were based on rigid body scattering theory. First ideal echoes were computed. Later it was found that by introducing some random phase shift into the return* that the target strengths could be made to agree more closely with the experimental data of Leiss [Ref. 2]. Calculations made for four hull types showed that the target strength initially increased with increasing jitter but then approached a constant upper bound as the jitter increased still further. For three of the hulls studied this constant value was in good agreement with the experimental data. The calculations for the fourth hull did not show good agreement with measured values.

*This random phase shift will be called "jitter."

While this technique usually provided good estimates of target strength (as well as realistic-looking echo signatures) based on the simplified approximate shape for the hull and sail, the introduction of an arbitrary jitter without a physical basis results in an inadequate foundation for understanding the mechanism for echo formation and, therefore, a poor basis for accurate prediction. The reason for the fourth hull to fail to agree with experiment was similarly not understood. Attempts to improve these inadequacies resulted in a further report [Ref. 3] in early 1972.

The work done during that project had two specific aims:

1. To describe a physical basis for the jitter phenomenon so that proper selection of the jitter parameter could be made based on the environmental factors; and

2. Upgrade the target strength program so that more complex geometry for the submarine could be used. Since it was felt that many submarine structures could not be adequately described with the simplified geometry used, and that this simplified geometry was perhaps the cause of the poor target strength results of the fourth hull.*

Progress was made in accomplishing both of these goals. A physical basis for selecting the jitter parameters was determined, the details of which may be found in Section II of Ref. 3. The waveform which results from reflections from the sea

*The hull in question has a special baffle for shielding special arrays from internal machinery noise. Such baffles are not present on the other hulls.

surface has a structure which includes Gaussian random time delays similar to the jitter which had been used previously in the program. This arrival delay time distribution depends upon the environmental sea state, wind speed, and velocity profile. It was also found during the work on the investigation of the arrival delay time distribution that the delay time is correlated along the target, and that this correlation can be characterized by a vertical correlation length and a horizontal correlation length. Unfortunately, not enough data are available to be able to find the dependence of these two correlation parameters on the environmental factors of sea state, wind speed, and velocity profile.

The jitter factor was found to be a linear function of the Rayleigh parameter, $k\sqrt{\overline{H}^2} \sin \psi$, where k is the wave number $(2\pi)/\lambda$ (λ is the wavelength of the sonar), $\sqrt{\overline{H}^2}$ is root-mean-square wave height, and ψ is the incidence angle of the sonar wave (measured from the horizontal surface to the direction of wave travel). This linear dependence holds from the Rayleigh parameter value of zero (where the jitter would also be zero) to a value of Rayleigh parameter of 0.7 (where the jitter becomes 0.5 radians, or 0.16 wavelengths). At this point, the jitter saturates; i.e., for higher values of the Rayleigh parameter the jitter no longer increases but remains at its saturated value of 0.16 wavelengths.

Additional geometry options were added to the program. The options added include cones and hemispheres:

1. Cone-shaped structures can be included in the hull description. These cones must have their axes coincident with the centerline of the hull. The position of the bases could be arbitrarily placed along the length and either cone face could be placed either fore or aft. The base radii of the truncated cone and the length of the cone are also input values. This option is

used when the ellipsoidal approximation to the hull shape is not adequate. Only the conical surface of the cone contributes to the reflection; the bases are ignored.

2. Hemispheres may also be used. Their position (three dimensions in location) may be specified as well as their radius, but the orientation must be such that the base is horizontal (with the submarine upright). The hemisphere may either be above or below the base. As with the cones, the reflecting surface is restricted to the hemispherical surface; the base is not included in the reflections. This option is used to account for the hemispherical caps of missile tubes on missile launching submarines. It may also give a better approximation to the bow shape of certain boats. It is assumed that none of the structural elements of ellipsoids, sail, cones, and hemispheres shade each other; so each element reflects independently.

The report [Ref. 3] shows several echoes as calculated from the program for a particular submarine at several aspect angles and for several combinations of jitter factor and longitudinal (horizontal) correlation length. The effects on the echo are clearly shown. Target strength probability distributions (plots of probability that the computed target strength will be less than T plotted against T) are also given. Because of the jitter, which appears in a Gaussian random form, the target strength varies from ping to ping and so such distributions exist for any aspect angle, and one can also draw such a distribution to integrate the data at all aspect angles.

This report extends the earlier work in the investigation of target strength. Jitter and correlation values were varied around physically indicated values in establishing echoes and the results compared to experimentally-determined curves. In addition, the effects of superposing the echoes from different

propagation paths were investigated and these results were also compared to the experiments.

In addition to calculating the echo returns from essentially "bare" hulls, calculations were made of echoes from boats which were coated to varying extents with acoustic absorbers on the hull and sail. The results of the calculations were compared to results obtained with the bare hull, and the effects of coating the submarine with acoustic absorbers on the sonar echo signature and target strength were determined.

II. CALCULATION OF TARGET STRENGTH

An outline of the theory on which the target strength computations are based will be given here. For a more detailed explanation, Ref. 4 may be consulted. The analysis is based on several assumptions:

1. Rigid Body Assumption - The body is assumed to be rigid so that the derivitive of the pressure in the direction of the normal to the surface is zero.

2. Kirchhoff Approximation - It is assumed that each element of area on the surface of the reflecting body radiates uniformly throughout a solid angle of 2π steradians.

3. Plane Wave Approximation - It is assumed that the range from the source to the target is large enough (compared to the target size with respect to the wavelength) so that the section of the spherical wave intercepting the target subtends a small solid angle and can accurately be approximated by a plane.

With these assumptions the reflected pressure, ΔP_r, at the receiver (located at the same place as the transmitter) due to the echo from the section of body located at x and of thickness Δx, where Δx is small compared to the wavelength, can be written

$$\Delta P_r = - \frac{iPf}{cx^2}\left[\exp[2\pi if(t - \frac{2x}{c})]\right]\iint_S \cos\psi \, dS$$

for the incident spherical wave whose amplitude is P, i.e.,

$$P_i = \frac{P}{x} \exp[2\pi if(t - \frac{x}{c})] \ .$$

The frequency is f, c is the sound speed, and ψ^* is the angle between the incident wave axis and the normal to the element of surface dS. The integral is performed over the area between x and $x + \Delta x$. It can be seen that this integral is the projection of the area in the direction from which the incident wave is coming; i.e., on the plane of the incident wave front.

Let A_n denote the projected area of the slice (small compared to λ^2, but finite) located at x_n. Then the echo from a target divided into M slices will be:

$$P_r = - \frac{ifP}{c} \sum_{n=1}^{M} \frac{\exp[2\pi if(t - \frac{2x_n}{c})}{x_n^2} A_n .$$

In the usual case (the one considered here) the transmitted pulse is finite, say of time extent τ. The reflected pulse will then be of extent $(2L)/c + \tau$, where L is the length of the target. The beginning of the return corresponds to the reflection from the closest slice on the target of the leading edge of the pressure wave. The echo ends with the reflection from the last slice which has a forward (toward the receiver) projected area of the trailing edge of the wave. At intermediate points the return is a sum of the reflections from several slices reflecting different portions of the wave, but in such relationship that the returns from these several slices are received simultaneously. The length of target which contributes to the return at any instant is $(c\tau)/2$, though some of this length may not be target; it may be some portion of the (nonreflecting) fluid in front of or behind the target.

---

*ψ is defined here differently from the ψ used earlier to determine the Rayleigh parameter.

Let the echo be represented by a series of samples, S_k, $1 \le k \le N$, and let the time increment be $(2\Delta x)/c$. This is the time delay between echoes from the same portion of the pulse from adjacent slices, Δx, of the submarine. The shape of the echo (disregarding amplitude scaling with transmitted pressure amplitude, frequency, sound speed, and range) can be represented by the series S_k where:

$$S_k = \sum_{n=1}^{k} A_{(k+1-n)} \sin\left(\frac{2\omega}{c} n\Delta x + \varphi\right) ,$$

where ω is the frequency in radians per second ($\omega = 2\pi f$), k satisfies $1 \le k \le M + N - 1$, where M is the number of slices into which the submarine is divided ($M = \frac{L}{\Delta x}$), N is the number of divisions (or slices) into which the pulse is divided, $N = \frac{c\tau}{\Delta x}$, and it is assumed that A_n is zero for $n > M$. The angle φ is the phase delay corresponding to two-way travel time (φ may be ignored for a single propagation path). For a sampling rate of m samples per cycle of the transmitted pulse, the slices must be such that

$$\Delta x = \frac{\lambda}{2m} = \frac{c}{2fm} .$$

The target strength of a submarine is defined as

$$T = 10 \log \frac{I_r}{I_i} ,$$

where T is the target strength and I_r and I_i are the reflected and incident intensities, respectively. In the case of a sinusoidal incident wave with an integral number of cycles, the target strength may be written as

$$T = 10 \log \frac{2}{\tau} \int_{t_o}^{t_o+\tau} e^2(t)dt ,$$

where e(t) is the radiated pressure (at one yard from the submarine center), and t_o is chosen to maximize the integral.

The above calculations can be made as described for both echo signature and target strength. The echoes thus generated are not realistic in appearance, and this also brings doubt as to the accuracy of the target strength predictions. The calculations described above are based on a homogeneous transmission path. To account for the inhomogeneous transmission field, the irregular surface of the water, and the fact that the target is not as smooth as the model, jitter, with or without correlation, has been introduced. Each slice of area is divided into a number of parts (the number may be one) and each is assigned a phase (time or distance) delay or advance, selected randomly from a Gaussian distribution with zero mean and with standard deviation called the jitter. The amplitude of the jitter is a function of the environmental conditions. This essentially moves each portion of the area for the calculation independently either forward or aft of its actual position, and the calculations of echo and target strength are based on this new distribution of areas. The effect on the echo is to make it more irregular, blur the changes in echo amplitude near the large scattering centers on the submarine (e.g., the sail), and decrease the maximum amplitude of the echo. The jittered echoes now vary on a ping-to-ping basis (using different random numbers for the calculation) as does the target strength. This is certainly more in agreement with experiment.

If no correlation is used (or if the correlation length is set to zero), then the phase shift applied to each portion of the area corresponding to each slice is based solely on a single random number and is independent of any other phase shift. If an in-plane correlation is used, then the area is divided into a number of segments with every other segment independent with intervening segments given the average value of the phase shift of the

two adjacent sections. For longitudinal correlation, each succeeding area section has a fraction of the phase shift of the previous area section. The fraction is determined so that the effect of a given random phase is reduced by the factor 1/e at a number of slices further away equal to the correlation length.

In addition to calculating single path echoes, including jitter and correlation, the program now has the capability to simulate echoes from more than one transmission path. In particular, four paths (for a single transmitted pulse) seemed to be a realistic assumption: a direct transmission and reflection (this path will have a very small jitter value), a direct transmission with a surface bounce return (this path will have a jitter based on the environmental conditions at the surface), a surface bounce transmission with a direct return path (this has the same jitter value as the previous single source path), and a surface bounce transmission and surface bounce reflection (this has double the jitter of a single surface bounce path). The echoes along these paths are added coherently, but they have a randomly-determined phase shift among them of up to one cycle, plus a phase shift of some integral number of cycles determined by the difference in path length.

The modifications made for absorber coatings is very straightforward. The area covered by absorber is assumed to reflect in the same way as a rigid body except that only some fraction of the energy is reflected; the rest is assumed to be absorbed. The coated area thus is effectively some smaller reflecting area than it would be were it not coated. The reflectivity may range from zero to one hundred per cent.

The output from the programs provides both the echo signature and the target strength. The echo shape can be compared to experimental shapes, but near matches should not be expected, as

both the experimental and computational echoes vary from ping to ping. They should show the same structure, indicating which features of the submarine are significant in forming echoes and, thus, are large contributers to the target strength. The target strength itself is an output of the program, and like its experimental counterpart, it also varies from ping to ping. The target strengths at a given aspect angle can predict the average target strength at that aspect angle as well as the expected variation. A more interesting use of the data is to gather the target strengths at all aspect angles without averaging any of them. These may be used to plot probability distributions of target strength. The experimental curves may be compared to the computed curves and this should give a good indication of the accuracy of the calculations. One can observe the effect of varying the input parameters on the shape and level of this curve.

One further presentation of data can be made. The average target strength, and its expected variation, can be displayed as a function of aspect angle.

The effects of acoustic absorber coating can also be shown on data presentations of the above types. These can show the usefulness or lack thereof of such coatings, as well as under which conditions they are most and least effective, and on which part of a submarine they are best used.

III. SAMPLE SUBMARINE CALCULATIONS

The program was exercised extensively for a typical nuclear, missile submarine. The geometrical description included the elliptical hull, the box with hemicylindrical end caps for the sail, five cones to approximate the pressure hull including the wasp waist, and a number of hemispheres to simulate the missile tube caps. The runs included calculations with different values of jitter and correlation, runs with multiple transmission paths, and runs with some of the submarine coated with acoustic absorbers.

There exist experimental data on this submarine obtained by Leiss and reported in Ref. 2. The ensonifying signal used in the experiments and in the calculations differs in two respects: the frequency and the pulse length. Target strength is essentially independent of frequency except through the effect of frequency on the Rayleigh parameter. For the calculations, the Rayleigh parameter was based on the experimental value of frequency, rather than the frequency used in the calculations. This would be equivalent to using a different sea state for the computational frequency. This frequency was about one-sixth that used for the experiments to reduce computer time. Similarly, the pulse length was reduced to 18 cycles, about 5 milliseconds. The target strength becomes independent of pulse length if the pulse length is larger than the target. If some smaller feature of the target (say the sail in the case of a submarine) is the primary contributor to the target strength, then it is only needed that the pulse be longer than this feature. It may be that the chosen pulse length is too small for accurate matching of the experiment at near bow aspect angles.*

*The measured target strengths were obtained with longer pulse lengths. In view of the sail dimensions, the measured target strength which should be compared with the 5 msec pulse computed target strength should be reduced by less than 2 dB in the worst cases (small aspect angles).

Choosing an appropriate value for the correlation lengths was made difficult by the scarcity of data. Only one paper [Ref. 5] has any information on this and gives data for one condition only, with no means of scaling with environment, frequency, or pulse length, all of which probably affect the value. Cases were run with the value of longitudinal correlation suggested by this report. The physical correlation length was kept identical, i.e., the number of meters, and, therefore, the correlation length expressed in terms of wavelength changed. This value was varied to search for better agreement with the experimental data and to determine output (echo shape and target strength) sensitivity to this parameter. The in-plane correlation was chosen so that the area of each slice was divided into five parts, three of which are totally independent and the other two obtained by averaging.

For proper scaling, the jitter factor was obtained by computing the Rayleigh parameter for the experimental conditions. This value was in the saturation regime and so the jitter factor was taken as its saturation value, or 0.08 wavelengths, assuming a single surface bounce in the two-way path. For a two-surface bounce, i.e., a surface reflection on both transmission and return, twice this amount of jitter is used (0.16 wavelengths). Since this jitter is applied to the computational frequency rather than the experimental frequency, it corresponds to a different amount of physical displacement of area sections within the echo. As with correlation length the value of jitter was also varied (from run to run) to observe the effect of changes in this parameter on the echo and particularly the effect on the target strength as exhibited on probability curves.

Table I shows a summary of the cases which were run. The case numbers are for reference only. The values shown in the column marked "C" are the correlation lengths used and are the

TABLE I

SUMMARY OF CASES

Case Number	C	J	Figure	Case Number	C	J	Figure
1	12	0.015	1	8	1	0.08	2,4
2	12	0.03	1	9	1	0.32	2
3	12	0.08	1,4	10	0	0.08	3,4
4	12	0.16	1	11	0	0.32	3
5	6	0.08	4	12[1]	1	Multi-path	5
6	3	0.08	4	13[2]	12	0.03	6
7	1	0.02	2	14[3]	12	0.03	6

Notes:

1. This case used four independent paths with C = 1 for all paths; one path had J = 0.01, two paths had J = 0.08, the fourth path had J = 0.16.

2. This case had its hull coated with 70% effective acoustic absorbers on an equal thickness strip which covered 90° of central angle at midship and extended to both ends.

3. This case had the sail coated with 70% effective acoustic absorbers.

number of wavelengths in the correlation length. The column marked "J" gives the jitter factor in radians and is the standard deviation of the zero mean value Gaussian distribution from which random numbers are chosen to jitter the phase of the return from each area. The column marked "Figure" shows in which figure (or figures) the results of that run are displayed. Cases 1 through 11 are single path returns with the correlation and jitter values as shown. Case number 3 is the case for which the best a priori estimates of correlation length and jitter for a single surface bounce are used. Case number 4 uses the best a priori estimates of these two parameters for two surface bounces--one in transmission and one in return. Case 5 also uses a close estimate of correlation length and the best estimate of jitter for the single bounce case.

Case number 12 differs from the other cases in that it is not a single path case. This case superposes the returns of four paths: a direct transmission with a direct return, a direct transmission with a single surface bounce return, a single surface bounce transmission with a direct return, and a single surface bounce transmission with a single surface bounce return. The jitter used for the first path is 0.01 wavelength to nominally account for nonhomogeneities in the water and nonsmoothness of the submarine. The jitter factor for the second and third paths is 0.08 wavelengths, based on the Rayleigh parameter for the environmental condition and a single bounce. The fourth path had a jitter factor of 0.16 wavelengths, based on the same environmental conditions as the second and third, but with two surface bounces, half of the jitter due to each bounce. The correlation length for this case was one wavelength. This value was chosen because it seemed to give the best agreement between the slope of the calculated target strength probability distribution and the experimental distribution (at least near the 50% probability point). The echoes from these paths were added coherently, but the relative time of arrival was chosen randomly uniform over one cycle.

Cases 13 and 14 were single path cases, but in these cases acoustic absorbers coated some portion of the submarine. For case 13 the absorber was placed on the hull. It was a straight strip bordered on top and bottom by horizontal planes. The width of this strip is such that it subtends a central angle from the longitudinal axis of 90° on each side of the boat at its midsection. As the cross section of the submarine decreases in radius away from the center section, the angle subtended by the absorber strip increases until at some point near the bow (and a point near the stern) it coats the entire cross section and does so for the remainder of the submarine. For case 14 the absorber is placed over the entire sail and no absorber is placed on the hull.

Figures 1 through 6 show the target strength distribution, the probability that target strength is less than T plotted against T. Except for Fig. 6, all curves are normalized so that the zero dB point is at the 50% probability point of the experimental curve. Figure 6 uses the 50% probability point of the computational uncoated boat as the zero dB point. This normalization is employed since it is only the comparison of experimental and variously computed curves that is of interest here, and not the actual levels of target strength. If the agreement between these curves is good, it is a simple matter to remove the normalization and return to actual target strength levels since only a shift in axis is used. The experimental curves are based on all aspect angles. The computed curves only cover one quadrant, from bow on to broadside, but it was felt that since the model used is nearly symmetric, this would be sufficient.

Figure 1 shows a group of curves of computed distributions for single paths, all with the same correlation length (12 wavelengths). They differ only in jitter values, which are 0.015, 0.03, 0.08, and 0.16. The experimental curve is shown also.

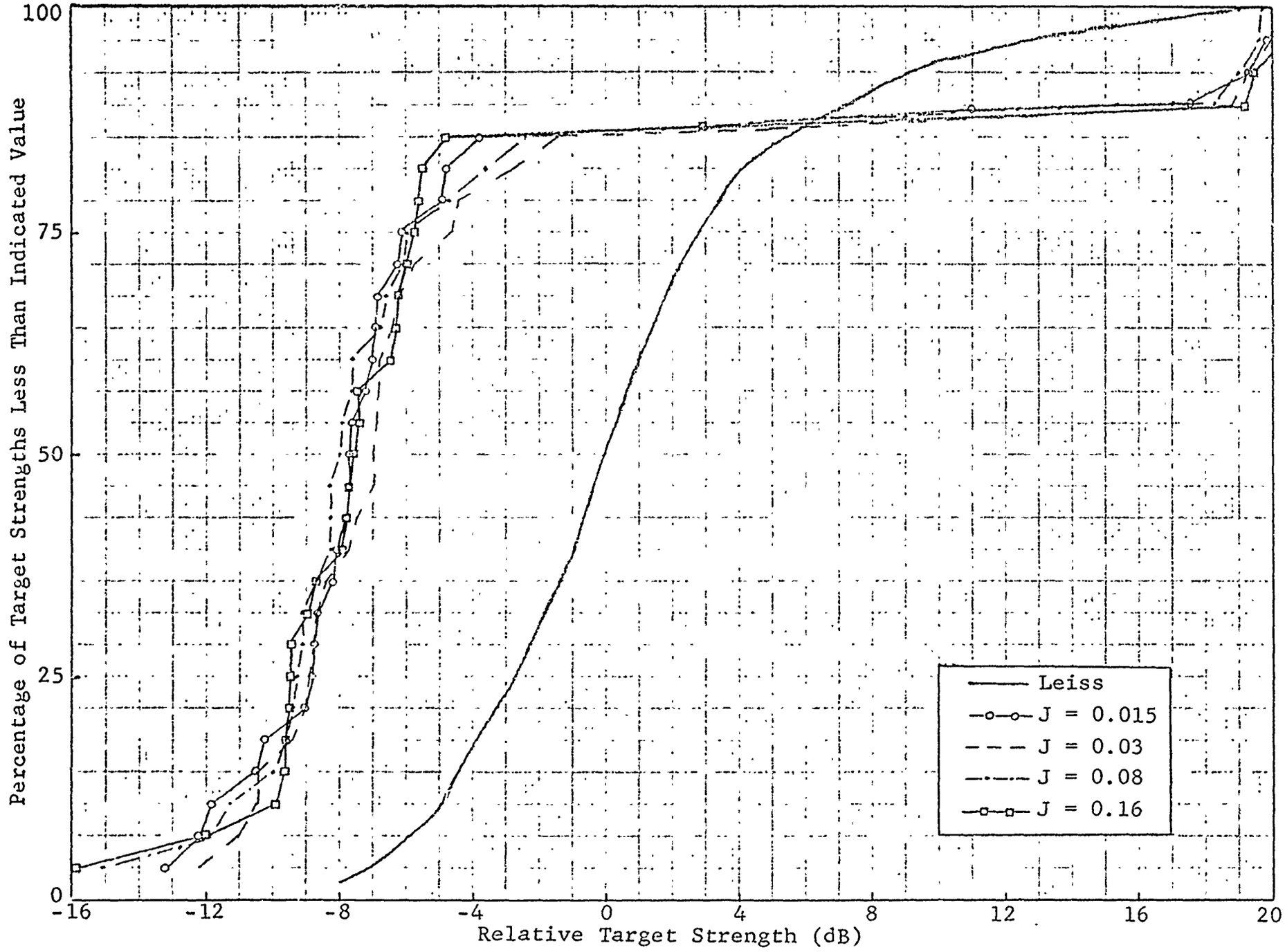

FIG. 1 - SINGLE PATH TARGET STRENGTH DISTRIBUTIONS FOR BARE HULL (C = 12λ, CORRELATION DISTANCE)

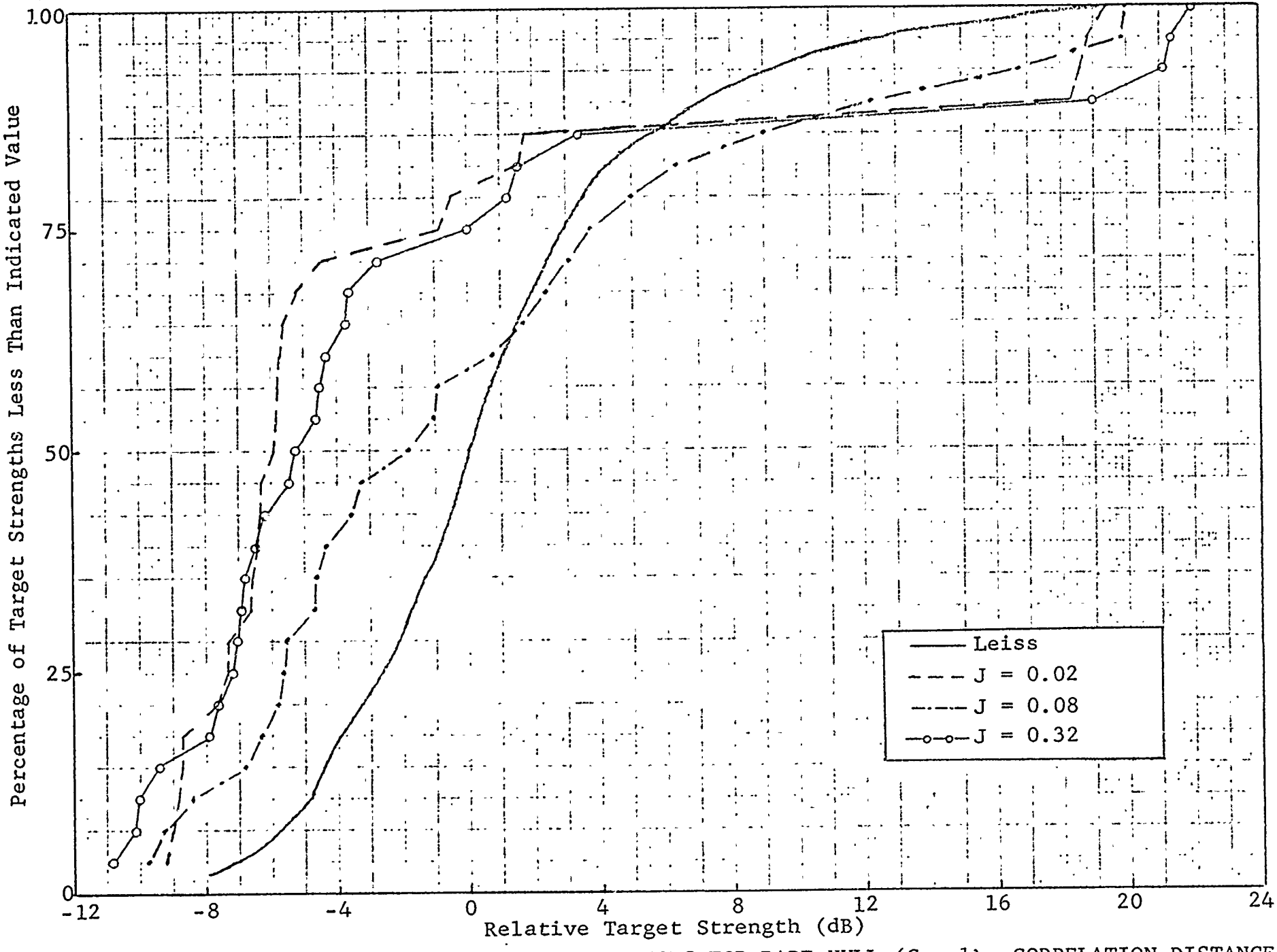

FIG. 2 - SINGLE PATH TARGET STRENGTH DISTRIBUTIONS FOR BARE HULL (C = 1λ, CORRELATION DISTANCE)

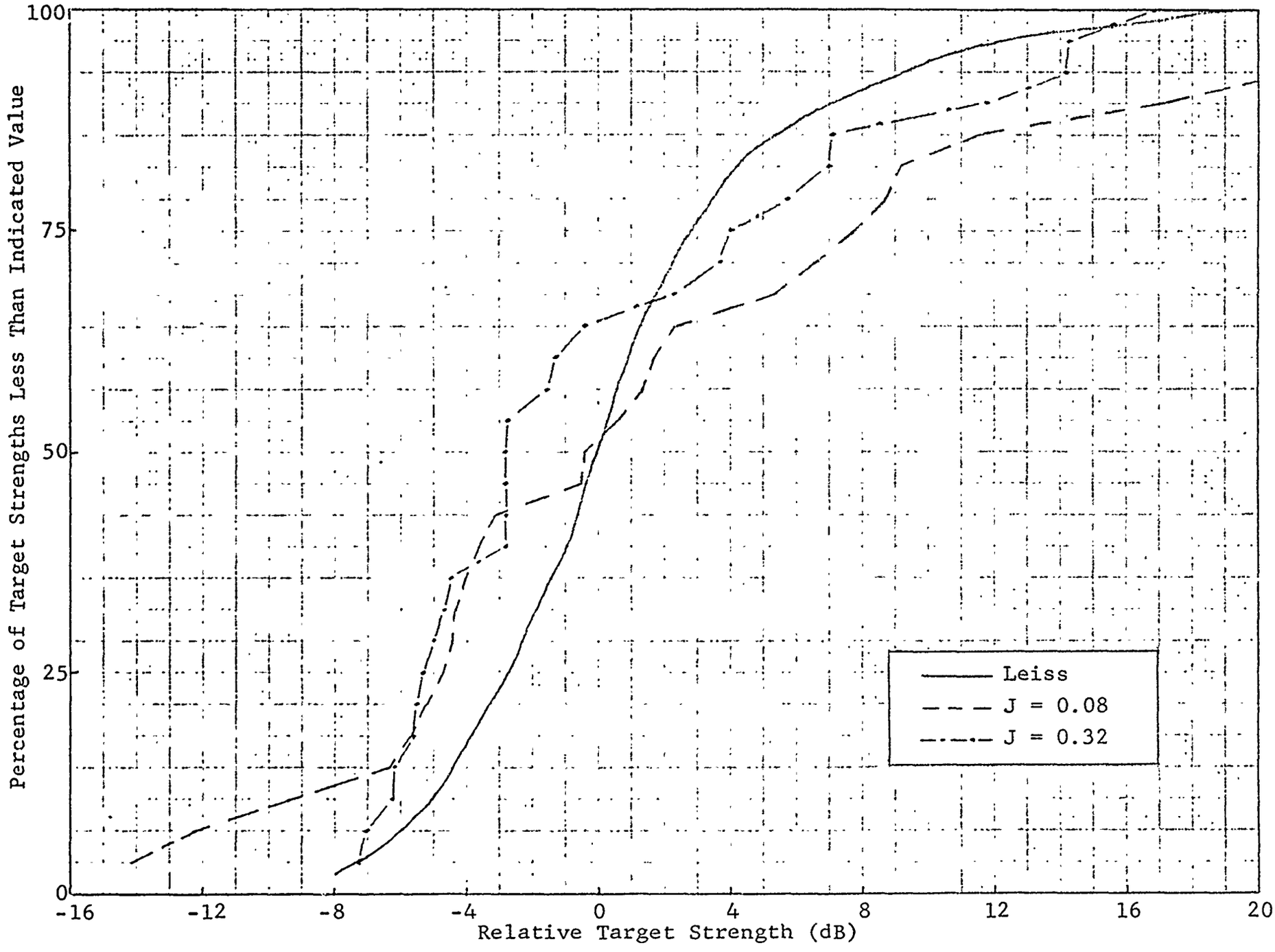

FIG. 3 - SINGLE PATH TARGET STRENGTH DISTRIBUTIONS FOR BARE HULL (C = 0, NO CORRELATION)

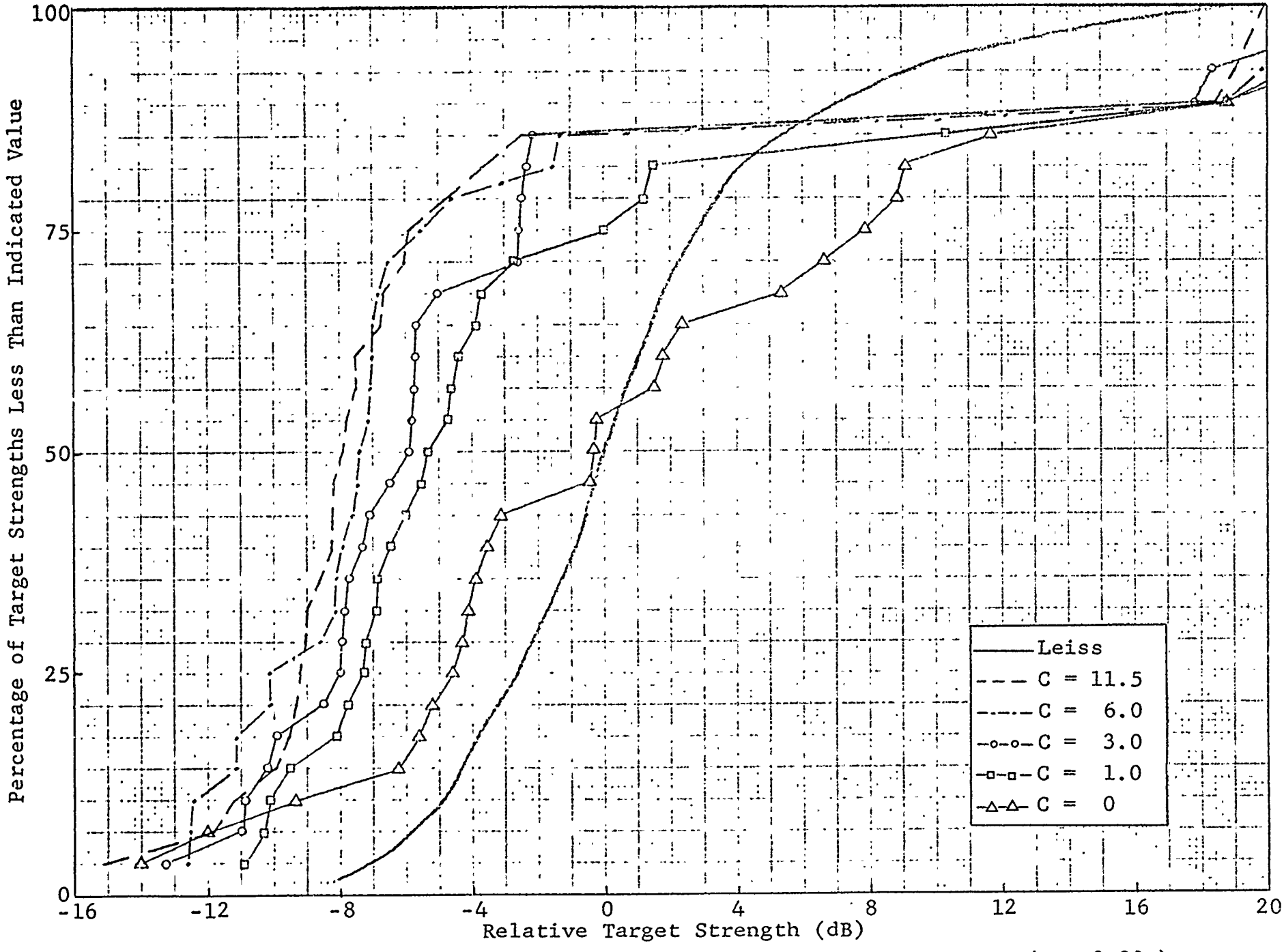

FIG. 4 - SINGLE PATH TARGET STRENGTH DISTRIBUTIONS FOR BARE HULL (J = 0.08λ)

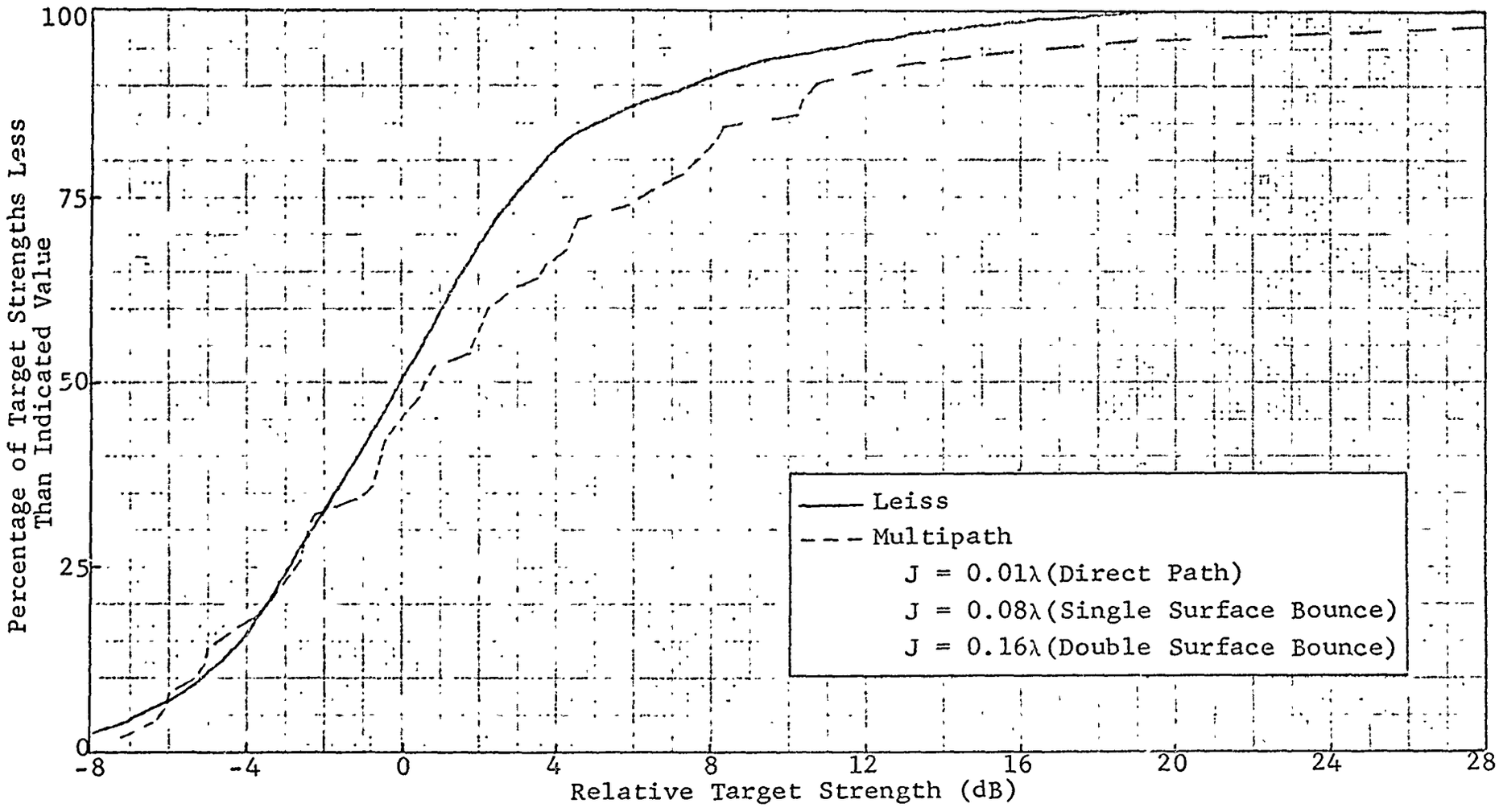

FIG. 5 - MULTIPATH TARGET STRENGTH DISTRIBUTIONS FOR BARE HULL (C = 1λ, CORRELATION DISTANCE)

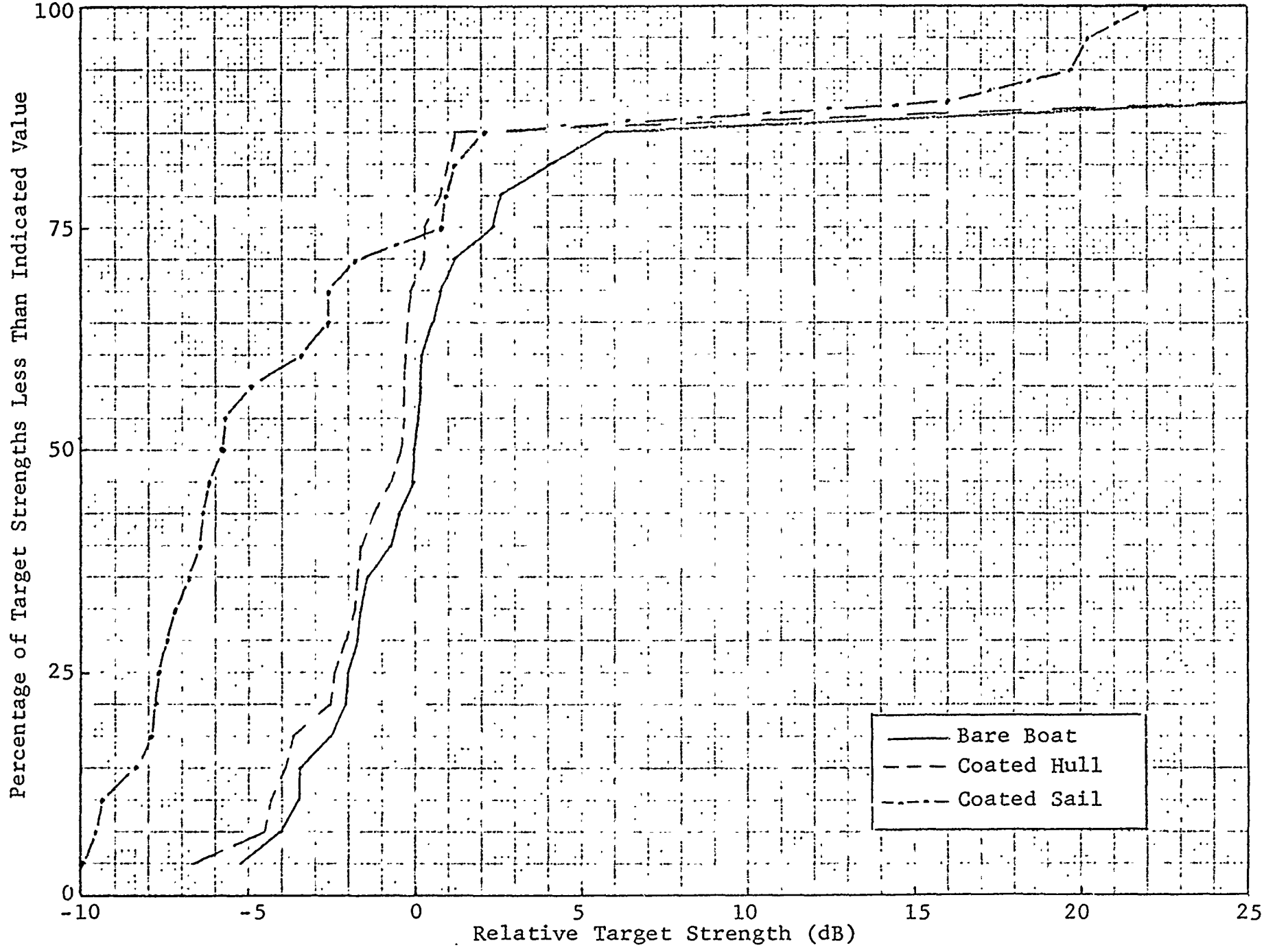

FIG. 6 - SINGLE PATH TARGET STRENGTH DISTRIBUTIONS FOR PARTIALLY COATED AND BARE SUBMARINES (J = 0.03λ)

It can be seen that for this value of correlation length that all of the curves are very similar, so that it seems that for this correlation length the distributions become almost independent of the jitter value. These computed curves are all about 7 dB lower at the 50% probability point than the experimental curve. Their slope, however, at this point (in percent per dB) is about 13½%/dB as compared to about 9%/dB for the experimental curve; they are, thus, fifty percent steeper.

Figure 2 presents computed distributions for single paths for a correlation length of one wavelength, again with the experimental distribution shown for comparison. The jitter values used for these curves are 0.02, 0.08, and 0.32. It can be seen from these curves that for this greatly reduced value of correlation length that the changes in jitter value become significant. For the lowest jitter value, i.e., 0.02, the 50% probability occurs at about 6 dB below the experiment; for the intermediate value, 0.08, which is the theoretically correct value, the 50% probability point is about 5 dB below the experiment; and for the highest jitter value, 0.32, (actually larger than the theoretical maximum based on a saturated Rayleigh parameter), the 50% probability point is only 2 dB below the experiment. The slopes of the curves also change significantly with jitter. The low jitter value has the steepest slope (at the 50% point) which is about 15%--much steeper than the experimental curve; the "right" jitter (0.08) curve has a slope of about 10%, which is very close to the experimental value; and the high jitter curve has a slope of about 4½%, much less steep than the experimental curve. The predicted jitter, therefore, seems to provide a distribution with the right slope. The single path may be responsible for the difference between the computed and experimental median values.

Curves showing the results of computations where the correlation length was zero (no correlation) are shown in

Fig. 3. The curves are for jitter factors of 0.08 and 0.32. The curve for the lower jitter comes within 1 dB of the experiment at the 50% probability point, but its slope of about 5½% at that point is too shallow. The curve for the higher jitter factor is 3 dB too low at the 50% probability point, while its slope at this point is only slightly too steep at 11%.

Figure 4 shows curves for a jitter factor of 0.08, the value based on the Rayleigh parameter for the experimental conditions and a single bounce path. The correlation lengths are 12, 6, 3, and 1 wavelengths, and a curve for no correlation. It can be seen that as the correlation length decreases, the level of the return increases and approaches the correct value (at the 50% probability point) as the correlation length approaches zero. As the correlation length decreases it can also be seen that the slope decreases.

It seems difficult to accurately match both the slope and level of the curves to the experimental curve by varying only the jitter factor and the correlation length, at least using the target geometry selected for these tests. Since a correlation length of one wavelength seemed to give the best agreement in slope with the theoretically correct jitter factor, this value was selected for superposing the four possible transmission-return paths which are present in the echo forming process. For this computation the jitter factor 0.01λ for the direct path, 0.08λ for each of the single surface bounce paths, and 0.16λ for the double surface bounce path were selected. This case is shown in Fig. 5. This is clearly the best match to the experimental distribution of all of the computational curves. The largest deviation in this case, and in most of the others, is at the high end of the scale where the computations predict much higher values of target strength. This occurs even for cases where the level is very low at the 50% probability point. These high target strength values occur at the broadside aspect and

are due to the sail model which has flat sides which give a very large return when perpendicular to the direction of the transmission and return. It is suggested that an improvement in the sail geometry be made.

Figure 6 shows the distributions computed for submarines with some acoustic absorber coating, as well as a case with no absorber coating for comparison. All cases used a jitter factor of 0.03* and a correlation length of 12 wavelengths--these values chosen to minimize the effect of jitter while still having some jitter present and so as to emphasize the effect of the absorber. The effect of placing acoustic absorbers over much of the hull only decreases the target strength at the 50% probability point by about one-half dB. This surprising result means that the sail return dominates the target strength at most aspect angles. Fully coating the sail alone, however, decreases the target strength at this point by about 5 dB, a significant amount. It seems then that the major contributor to the target strength is not the outer hull nor the pressure hull, but the sail. After coating the sail, it is found that the sail return is still slightly larger than the hull return.

*The work described in this report proceeded in parallel. It was not apparent at the outset that J = 0.08λ would have been a better choice for this part of the study. Nevertheless, changes in target strength which can be produced by coating will not be seriously altered by changes in the jitter factor.

IV. CONCLUSIONS AND RECOMMENDATIONS

The first and most important conclusion that can be made from this investigation is that the method used is essentially valid, that realistic echoes can be formed, and that target strengths can be accurately predicted if the proper choice of parameters can be made. At this point the most accurate predictions are being made with an overlay of several acoustic paths through the water. Unfortunately, this increases the calculation time since the signature calculations take much more time than the calculations which generate sectional areas from the geometry. It would be useful if the multiple path return could be simulated in some way without having to actually compute the processed signals for four paths. It would also be quite useful and time saving if the echo could be varied from its nominal unjittered shape directly from the set of random numbers that are used for the jitter.

Secondly, it can be seen from the figures that the sail plays a significant part in echo formation and is the dominant influence on target strength. This can also be seen on typical echoes by comparing echo maxima with corresponding position on the submarine. The role of the sail in the calculations would probably be reduced and brought more into line with experiment (note the influence of the sail on values of the curves at high probabilities) if a more accurate geometric description were made. It would seem, in fact, at this point, that the weakest point of the target strength prediction program is the geometrical description of the target, in particular the description of the sail, and that important improvements could be made in the accuracy of the predictions if a better geometrical description of the outer hull, pressure hull, sail, and other details of the target could be made.

The third conclusion to be made is that it can be seen that the effects of acoustic absorbers can be large or small,

depending on how they are used. When a better geometrical description of the submarine is available, an efficient distribution of acoustic absorbers may be found by exercising the program with different placements of the coating. It is likely that significant reductions in target strength can be made by the proper use of acoustic absorber coatings.

Three theoretical investigations should be pursued. First, the effect on the echo of a pressure hull separated from the fairwater is not clear. An analysis which might clear this up would compare, for example, the scattered field of a rigid shell, say an infinite cylinder or a sphere, due to a plane wave, with a similar shell structure consisting of a thin shell enclosing a rigid internal shell with water between them, or a thin shell enclosing a thick but nonrigid shell filled with air, with water separating the two shells. Second, an investigation also ought to be made of the characteristics of an acoustic absorber to determine if the only effect is to absorb some portion of the energy, or if it also affects the reflection pattern, i.e., if the Kirchhoff approximation is still valid, if the absorber causes phase changes, and if the areas where absorber coatings and bare body meet cause any unaccounted for phenomena. Third, a good theoretical method to calculate the correct correlation lengths to use in the calculations should be found. This method should show the variation of correlation length with environmental conditions, sonar frequency, and pulse length.

V. REFERENCES

1. C. L. Kite, "Computation of Target Strength (U)," Summary Report, TRACOR Document 66-463-C, 17 November 1966, CONFIDENTIAL.

2. W. J. Leiss, "Submarine Target Strength Summary," University of Pennsylvania, Ordnance Research Laboratory, 1964.

3. B. M. Brown, J. J. Lobdill, and W. McKemie, "Target Strength Prediction," TRACOR Document T72-AU-9508-U, UNCLASSIFIED.

4. C. L. Kite, "Computation of Submarine Target Strengths (U)," TRACOR Document 66-463-C, 10 November 1966, CONFIDENTIAL.

5. E. P. Gulin and K. I. Malyshev, "Experiments in the Spatial Correlation of the Amplitude and Phase Fluctuations of the Acoustic Signals Reflected from a Rough Ocean Surface," Soviet Phys.-Acoustics, Vol. 10, No. 4, April-June, 1965, pp. 365-368.